

Dehydration, Micellization, and Phase Separation of Thermosensitive Polyoxazoline Star Block-Copolymers in Aqueous Solution

Tetiana Sezonenko,¹ Xing-Ping Qiu,² Françoise M. Winnik,³ and Takahiro Sato¹

¹ Department of Macromolecular Science, Osaka University, 1-1 Machikaneyama-cho, Toyonaka 560-0043, Japan

² Faculty of Pharmacy, Department of Chemistry, University of Montreal, CP 6128 Succursale Centre Ville Montreal, Quebec, Canada H3C 3J7

³ Department of Chemistry, University of Helsinki, P.O. Box 55 (A.I. Virtasen aukio1) FI-00014 Helsinki, Finland

Abstract:

Suitably end-functionalized diblock copolymers (2-isopropyl-2-oxazoline)-*b*-(2-ethyl-2-oxazoline) (PIPOZ-*b*-PEOZ) were linked to a tetrafunctional core in order to synthesize two isomeric thermosensitive 4-arm star block polymers which have the PIPOZ block near the core, core-(PIPOZ-*b*-PEOZ)₄, or near the outer surface the star polymer, core-(PEOZ-*b*-PIPOZ)₄. The solution properties of the star copolymers in water were monitored by turbidimetry, microcalorimetry, and small-angle X-ray scattering (SAXS). The dehydration and cloud-point temperatures of both core-(PIPOZ-*b*-PEOZ)₄ and core-(PEOZ-*b*-PIPOZ)₄ in water are in the vicinity of 50 °C. Above this temperature, core-(PIPOZ-*b*-PEOZ)₄ forms star-like aggregates, whereas core-(PEOZ-*b*-PIPOZ)₄ remains isolated, with no sign of aggregation. These results demonstrate the importance of chain architecture on the association of thermosensitive tetra-arm star block copolymers in water above the solutions phase transition temperature.

Key words: thermosensitive polymer, star block copolymer, dehydration, micelle, phase separation, small angle X-ray scattering

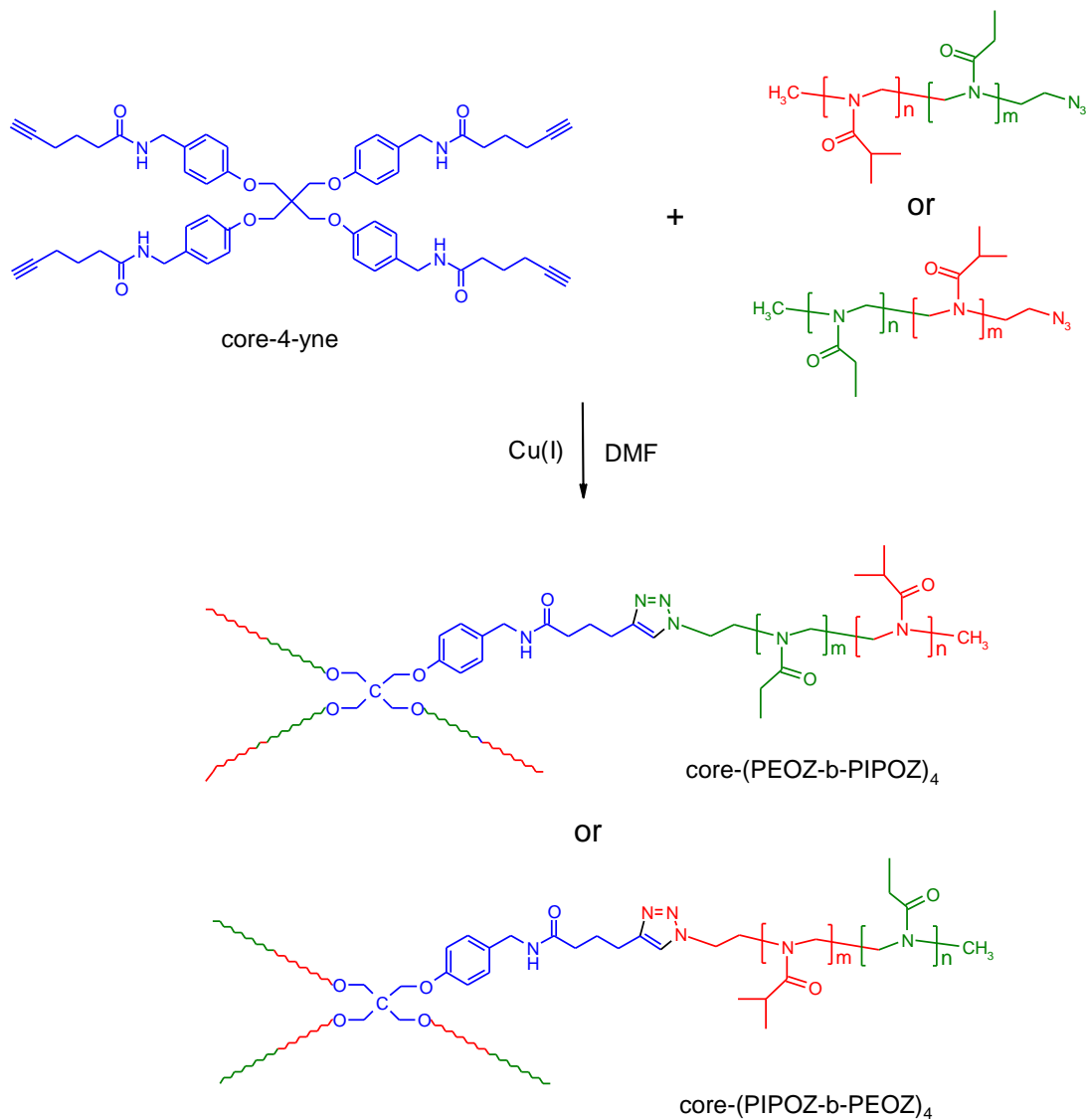
INTRODUCTION

Star polymers are versatile building blocks in the preparation of functional materials.¹ The functionality of the material is amplified by end-modification of the arms.^{1,3} In the case of core-modified star polymers, the arms stabilize, protect, or modulate the inner functionality.^{1,2} Stimuli-responsive star block copolymers are useful in various biotechnological applications, since their conformation and self-association can be controlled through changes in temperature^{2,4-7} pH,^{6,8-10} light,^{2,11} or ionic strength^{9,12}. There have been few studies so far on the effects of the star copolymers architecture on their conformation and intermolecular interactions in solution, although they are of fundamental importance and should be known in order to use the unique features of star copolymer most effectively.

Takahashi et al.¹³ have reported the effect of temperature on the dehydration, self-association, and phase separation behavior in water of diblock copolymers containing a poly(2-ethyl-2-oxazoline) (PEOZ) and a poly(2-isopropyl-2-oxazoline) (PIPOZ) block. Both PIPOZ and PEOZ are soluble in water below ca. 45 °C. The PIPOZ chains dehydrate between 45 and 55 °C, while PEOZ remains soluble in water, hence PEOZ-*b*-PIPOZ copolymers are amphiphilic in this temperature range. Above 55 °C, both PIPOZ and PEOZ are dehydrated and insoluble in water. It was observed experimentally that at 50 °C PEOZ-*b*-PIPOZ aggregation occurs with concomitant macroscopic liquid-liquid phase separation, whereas at 70 °C phase separation occurs without macroscopic phase separation.

Using PEOZ-*b*-PIPOZ diblock copolymers, we prepare via click coupling two isomeric tetra-arm star copolymers, [core-(PIPOZ-*b*-PEOZ)₄], in which the PIPOZ blocks are linked directly to the core, and [core-(PEOZ-*b*-PIPOZ)₄], in which the PEOZ block is linked to the core (cf. Scheme 1). These two star block copolymers were utilized to investigate the architecture dependences of the micellar structure as well as the dehydration and phase

separation behavior of the star copolymers upon heating. The micellar structure and dehydration behavior were investigated by small angle X-ray scattering (SAXS) and high-sensitivity differential scanning calorimetry (HS-DSC), respectively.



Scheme 1. Synthesis of core-(PEOZ-*b*-PIPOZ)₄ and core-(PIPOZ-*b*-PEOZ)₄ starting from the tetrafunctional moiety core-4-yne.

EXPERIMENTAL SECTION

Materials. All chemicals were purchased from Sigma-Aldrich Chemical Co. and used as received unless specified otherwise. 2-Isopropyl-2-oxazoline was synthesized from isobutyronitrile and 2-aminoethanol according to the synthetic protocol of Huber and

Jordan.¹⁴ The monomers, 2-isopropyl-2-oxazoline (IPOZ) and 2-ethyl-2-oxazoline (EOZ), were purified by vacuum distillation over calcium hydride. Dimethylformamide (DMF) and acetonitrile (AcCN) were purified by a solvent purification system with two columns packed with activated alumina provided by Innovative Technology Inc. Water was deionized using a Millipore MilliQ system.

Instrumentation, ¹H NMR spectra were recorded on a Bruker AMX-400 (400 MHz) spectrometer using chloroform-D (CDCl₃) as the solvent. The molecular weight and its distribution (PDI) of the polymers were measured with a GPC-MALLS system consisting of an Agilent 1100 isocratic pump, a set of TSK-gel a-M (particle size 13 μ, exclusion limit 1 × 10⁷ Da for polystyrene in DMF) and a TSK-gel a-3000 (particle size 7 μ, exclusion limit 1 × 10⁵ Da for polystyrene in DMF) (Tosoh Biosep) columns, a Dawn EOS multi-angle laser light scattering detector λ = 690 nm (Wyatt Technology Co.) and an Optilab DSP interferometric refractometer λ = 690 nm (Wyatt Technology Co.) under the following conditions: injection volume, 100 μL; flow rate, 0.3 mL/min; eluent, DMF; temperature, 40 °C. The specific refractive index increment $\partial n/\partial c$ of the diblock copolymer in DMF was calculated by $\partial n/\partial c = w_1(\partial n/\partial c)_1 + w_2(\partial n/\partial c)_2$ with w_1 and w_2 denoting the weight fraction of PIPOZ [$(\partial n/\partial c)_1 = 0.084$ mL/g] and PEOZ [$(\partial n/\partial c)_2 = 0.078$ mL/g] blocks, respectively.

Synthesis of the PIPOZ-*b*-PEOZ-N₃ diblock copolymer. The diblock copolymer PIPOZ-*b*-PEOZ-N₃ was synthesized by sequential cationic ring opening polymerization (CROP) of 2-isopropyl-2-oxazoline and 2-ethyl-2-oxazoline initiated by methyltrifluoromethanesulfonate in acetonitrile at 70 °C.¹⁵ A flame-dried flask equipped with a N₂-filled condenser and a rubber stopper was charged with dry acetonitrile (20 mL). The first monomer, 2-isopropyl-2-oxazoline (2.5 mL, 22.0 mmol), and the initiator, methyl triflate (50 μL, 0.44 mmol) were added in sequence at room temperature via N₂-filled syringes. The flask was immersed in an oil bath pre-heated to 70 °C. The polymerization was conducted at 70 °C for 3 days until monomer conversion reached ~95 %, as determined by ¹H NMR spectroscopy.

Then, the second monomer, 2-ethyl-2-oxazoline (2.5 mL, 25.0 mmol) was added and the polymerization was continued for another 2 days at the same temperature until the overall monomer conversion reached ~90%. Sodium nitride (NaN_3 , 0.3 g, 4.4 mmol) was added to quench the terminal oxazolinium groups. The termination reaction was conducted at 60 °C for 6 hours. Afterwards, the polymerization solution was cooled to room temperature and diluted with water to 100 mL. The resulting solution was dialyzed against deionized water for 3 days. The purified polymer was recovered by freeze-drying. Yield 4.0 g, 80%. ^1H NMR (CDCl_3 , δ) ppm: 1.10 (s, $-\text{CH}(\text{CH}_3)_2$), 2.32 and 2.42 (d, $-\text{CH}_2\text{CH}_3$), 2.69 and 2.91 (d, $-\text{CH}(\text{CH}_3)_2$), 3.45 (s, $-\text{NCH}_2\text{CH}_2-$); cf. Figure S1 in the Supporting Information.

Synthesis of the PEOZ-*b*-PIPOZ- N_3 Diblock Copolymer. The diblock copolymer PEOZ-*b*-PIPOZ- N_3 was synthesized by sequential CROP of 2-ethyl-2-oxazoline and 2-isopropyl-2-oxazoline as described above, except that 2-ethyl-2-oxazoline was polymerized first, followed by addition of 2-isopropyl-2-oxazoline (2.5 mL, 22.0 mmol); Yield 4.0 g, 80%. ^1H NMR (CDCl_3 , δ) ppm: 1.10 (s, $-\text{CH}(\text{CH}_3)_2$), 2.32 and 2.42 (d, $-\text{CH}_2\text{CH}_3$), 2.69 and 2.91 (d, $-\text{CH}(\text{CH}_3)_2$), 3.45 (s, $-\text{NCH}_2\text{CH}_2-$); cf. Figure S2 in the Supporting Information.

Synthesis of core-(PEOZ-*b*-PIPOZ) $_4$ Star Block Copolymer. Core-4-yne (19.6 mg, 0.02 mmol, 1 equiv.) and PIPOZ-*b*-PEOZ- N_3 (1.2 g, 0.16 mmol, 8 equiv.) were dissolved in dry DMF (15 mL). After degassing with N_2 for 30 min, N, N, N', N'' , N'' -pentamethyldiethylenetriamine (PMDETA, 17.3 mg, 0.1 mmol, 5 equiv.) and cuprous bromide (CuBr , 14.3 mg, 0.1 mmol, 5 equiv.) were added. The mixture was stirred at room temperature for 3 days. Afterwards, 15 mL of water was added and the solution was dialysed against deionized water for 2 days with a regenerated cellulose membrane (MWCO of 3.5 kDa). The solution was concentrated and purified by ultrafiltration using a Millipore 76 mm ultracel membrane (MWCO of 10 kDa) to remove unreacted PIPOZ-*b*-PEOZ- N_3 . The retentate was freeze-dried to obtain the star polymer core-(PEOZ-*b*-PIPOZ) $_4$ as a white solid. Yield 0.5 g, 80%. ^1H NMR (CDCl_3 , δ) ppm: 1.10 (s, $-\text{CH}(\text{CH}_3)_2$), 2.32 and 2.42 (d, $-\text{CH}_2\text{CH}_3$),

2.69 and 2.91 (d, $-CH(CH_3)_2$), 3.45 (s, $-NCH_2CH_2-$), 4.30 and 4.34 (d, $Ar-CH_2-NH-$), 6.84 (s, $Ar-H$), and 6.25 (s, $Ar-H$).

Synthesis of core-(PIPOZ-*b*-PEOZ)₄ Star Block Copolymer. The star block copolymer core-(PIPOZ-*b*-PEOZ)₄ was synthesized in the same way as the star block copolymer core-(PEOZ-*b*-PIPOZ)₄, starting from core-4-yne (19.6 mg, 0.02 mmol, 1 equiv.) and PEOZ-*b*-PIPOZ-N₃ (1.2 g, 0.16 mmol, 8 equiv).

High-Sensitivity Differential Scanning Calorimetry (HS-DSC). HS-DSC measurements were performed on a VP-DSC microcalorimeter (MicroCal Inc.) at an external pressure of ca.250 kPa. The cell volume is 0.520 mL. The polymer concentration was set to w (the polymer weight fraction) = 0.001, and the heating rate was set at 1.0 °C/min in the temperature range 10 – 80 °C. The experimental data were analyzed using the Origin based software supplied by the manufacturer. A cubic connect baseline was subtracted from the data prior to fitting.

Turbidimetry. Turbidities of aqueous star block copolymer solutions (the copolymer weight fraction $w = 0.001$) were measured by spectrophotometric detection of the changes in turbidity at $\lambda = 550$ nm on an Agilent 8453 UV-Visible spectroscopy system equipped with an HP 89090A Peltier temperature controller. The heating rate was 0.2 °C/min.

Phase Separation Observation. Aqueous solutions of core-(PIPOZ-*b*-PEOZ)₄ and core-(PEOZ-*b*-PIPOZ)₄ with a polymer weight fraction $w = 0.0244$ were placed in stoppered glass test tubes, and kept at 50 and 60 °C in a thermostated oven and monitored visually at various heating times.

Preparation of solutions for SAXS measurements

Small-Angle X-Ray Scattering (SAXS). SAXS measurements were conducted on aqueous solutions of the core-(PIPOZ-*b*-PEOZ)₄ and core-(PEOZ-*b*-PIPOZ)₄ samples with $w = 0.0244$ at 25, 40, 50, 60, and 70 °C, using the beamline 40B2 at Spring-8, Kobe, Japan. The test solutions were placed in capillary tubes. The capillary tubes were placed in a heating

block set at a constant temperature to ensure rapidly heating. The scattered X-ray intensities were measured using an imaging plate detector 3 min after the T-jump. A new test solution was used for each T-jump experiment to different temperatures.

The SAXS excess Rayleigh ratio $R_{X,\theta}$ at the scattering angle θ and the optical constant K_e of SAXS were calculated by^{16, 17}

$$R_{X,\theta} = F \left(\frac{I_{\theta,\text{soln}}}{I_{\text{mon,soln}}} - \frac{I_{\theta,\text{solv}}}{I_{\text{mon,solv}}} \right), \quad K_e = N_A a_e^2 \gamma_{\text{av}}^2 \quad (1)$$

Here, F is the instrument constant, $I_{\theta,\text{soln}}$ ($I_{\theta,\text{solv}}$) and $I_{\text{mon,soln}}$ ($I_{\text{mon,solv}}$) are the scattering intensity at the scattering angle θ and the monitor value of the incident SAXS intensity, respectively, of the solution (of the solvent), N_A is the Avogadro constant, a_e is the electron radius (2.8×10^{-13} cm), and γ_{av} is the average SAXS contrast factor of the copolymer. The value of γ_{av} for the copolymer in water was calculated by

$$\gamma_{\text{av}} = \frac{M_{w,\text{IPOZ}} \gamma_{\text{IPOZ}} + M_{w,\text{PEOZ}} \gamma_{\text{EOZ}}}{M_{w,\text{IPOZ}} + M_{w,\text{PEOZ}}} \quad (2)$$

with the molar masses $M_{w,\text{IPOZ}}$ and $M_{w,\text{PEOZ}}$, as well as the contrast factors for IPOZ and EOZ monomer units given by

$$\gamma_{\text{IPOZ}} = \frac{n_{e,\text{IPOZ}}}{M_{0,\text{IPOZ}}} - \frac{\bar{v}_{\text{IPOZ}} n_{e,\text{H}_2\text{O}}}{v_{\text{solv}} M_{\text{H}_2\text{O}}}, \quad \gamma_{\text{EOZ}} = \frac{n_{e,\text{EOZ}}}{M_{0,\text{EOZ}}} - \frac{\bar{v}_{\text{EOZ}} n_{e,\text{H}_2\text{O}}}{v_{\text{solv}} M_{\text{H}_2\text{O}}} \quad (3)$$

where $n_{e,i}$ and $M_{0,i}$ ($i = \text{IPOZ}, \text{EOZ}, \text{and H}_2\text{O}$) are numbers of electrons and molar masses of i , respectively, \bar{v}_i is the partial specific volume of the monomer unit i ($= \text{IPOZ}$ and EOZ), and v_{solv} is the specific volume of water. By density measurements of the copolymer samples, the partial specific volumes were determined to be $\bar{v}_{\text{IPOZ}} = 0.892 \text{ cm}^3/\text{g}$ and $\bar{v}_{\text{EOZ}} = 0.884 \text{ cm}^3/\text{g}$ ($\gamma_{\text{IPOZ}} = 0.0531 \text{ mol/g}$; $\gamma_{\text{EOZ}} = 0.0543 \text{ mol/g}$). Temperature dependences of γ_{IPOZ} and γ_{EOZ} were neglected.

Neglecting the inter-particle interference effect and the dispersity in the copolymer composition, the scattering function can be written as:

$$R_{X,\theta}/K_e c = M_w P_z(k) \quad (4)$$

where c is the copolymer mass concentration, M_w is the weight average molar mass, and $P_z(k)$ is the z -average particle scattering function. The instrument constant F in eq 1 was determined so as for the low angle $R_{X,\theta}/K_e c$ for the aqueous core-(PIPOZ-*b*-PEOZ)₄ at 25 °C to agree with $M_{w,1}$ ($= 2.42 \times 10^4$ g/mol) of the copolymer, determined by SEC-MALS (see Table 1 below).

RESULTS AND DISCUSSION

Synthesis of the Star Block Copolymers. The star copolymers were prepared by copper-catalyzed click coupling in DMF of a tetra-propargylated moiety (core-4-yne) to either PEOZ-*b*-PIPOZ-N₃ or PIPOZ-*b*-PEOZ-N₃, which were obtained by methyl trifluoromethane catalyzed sequential CROP polymerization of IPOZ and EOZ, or vice-versa (see experimental section and supporting data for the complete characterization of the copolymers). To ensure complete substitution of the core, the copolymers were added in a 2:1 molar ratio with respect to the alkyne groups of the core (Scheme 1). The mixtures recovered at the end of the coupling reaction were purified by extensive ultracentrifugation with a membrane permeable to the diblock copolymers, but not the tetra-arm stars. The purity of the recovered star copolymers was ascertained by gel permeation chromatography (see GPC scans in Figure S3). In Table 1, we give the composition and molar mass of the diblock copolymers and the tetra-arm star copolymers are presented in Table 1.

Table 1. Molecular characteristics of precursor PIPOZ-*b*-PEOZ samples and star block copolymer samples synthesized.

polymer	x_{IPOZ}^a	$M_{n,1}/10^3{}^b$	$M_{w,1}/M_{n,1}^c$	$M_{w,1}/10^3{}^d$ ($M_{w,1}/10^3{}^e$)	$N_{0n,\text{PIPOZ}}^f$ ($N_{0w,\text{PIPOZ}}^g$)	$N_{0n,\text{PEOZ}}^f$ ($N_{0w,\text{PEOZ}}^g$)
PEOZ- <i>b</i> -PIPOZ-N ₃	0.58 ₅	6.5	1.14	7.4 (7.4)	35 ^d (40 ^e)	25 ^d (29 ^e)

core-(PIPOZ- <i>b</i> -PEOZ) ₄		27	1.03	28 (24)	128 ^d (132 ^e)	91 ^d (94 ^e)
PIPOZ- <i>b</i> -PEOZ-N ₃	0.42	7.5	1.05	7.9 (7.9)	30 ^d (31.5 ^e)	41 ^d (43.5 ^e)
core-(PEOZ- <i>b</i> -PIPOZ) ₄		31	1.02	32 (31)	121 ^d (124 ^e)	167 ^d (171 ^e)

^a Mole fraction of IPOZ in the copolymer measured by ¹H NMR. ^b Number average molar mass of the copolymer in units of g/mol measured by ¹H NMR. ^c Dispersity index measured by SEC-MALS. ^d Weight average molar mass calculated from $M_{n,1}$ and $M_{w,1}/M_{n,1}$ in the third and fourth columns. ^e Weight average molar mass measured by SEC-MALS. ^f Number average degree of polymerization for the PIPOZ and PEOZ blocks. ^g Weight average degree of polymerization of the PIPOZ and PEOZ blocks.

The ¹H NMR spectrum of core-(PIPOZ-*b*-PEOZ)₄ in CDCl₃ (Figure 1) presents signals due to the resonances of protons of the core at 4.30-4.34 ppm (benzyl protons) and 6.84-7.25 ppm (aromatic protons) in addition to the signals due to the copolymers of the arms. The complete substitution of the core indicated by GPC measurements was validated by the relative intensity of the signals due to the protons of the arms and the core and the known composition of the diblock copolymers. The molecular formulae of the two star copolymers are core-(PIPOZ₃₅-*b*-PEOZ₂₅)₄ and core-(PEOZ₄₁-*b*-PIPOZ₃₀)₄, respectively. Based on the formulae, the M_n of the two star copolymers was calculated to be 26.8 and 30.8 kDa, respectively, in good agreement with the values measured by SEC-MALS (Table 1). The ¹H NMR spectrum of core-(PEOZ-*b*-PIPOZ)₄ is shown in Figure S4.

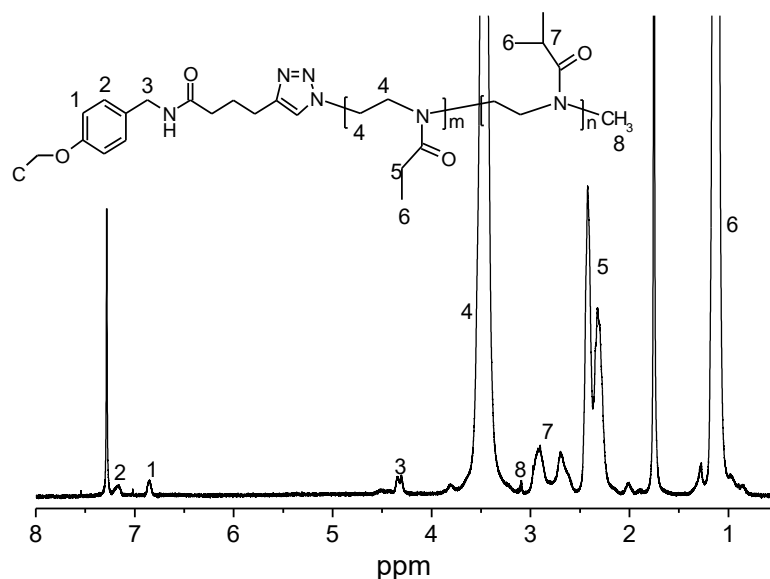


Figure 1. ^1H NMR spectrum of core-(PEOZ-*b*-PIPOZ) $_4$ in CDCl_3 .

HS-DSC Thermograms. The thermograms of aqueous solutions of the two star block copolymers feature a single endotherm (Figure 2) with maxima at 47.0 °C and 50 °C for core-(PIPOZ-*b*-PEOZ) $_4$ and core-(PEOZ-*b*-PIPOZ) $_4$, respectively. The mole fraction of IPOZ is slightly higher in core-(PEOZ-*b*-PIPOZ) $_4$, compared to core-(PIPOZ-*b*-PEOZ), which may account for the difference in the two T_m values. Also, the full width at half maximum of the endotherm recorded for aqueous core-(PEOZ-*b*-PIPOZ) $_4$ (= 7.7 °C) is slightly broader than in the case of core-(PIPOZ-*b*-PEOZ) $_4$ (= 6.6 °C), indicating that the dehydration temperature difference between the PEOZ and PIPOZ block chains for core-(PEOZ-*b*-PIPOZ) $_4$ may be slightly larger than that for core-(PIPOZ-*b*-PEOZ) $_4$. *The DSC thermograms for aqueous solutions of the two star block copolymers are compared with those for aqueous solutions of the precursor block copolymers in the Supporting Information.* Sato-san: I would like to show the DSC of the deblocks in the main text with a short description, or else not mention them all

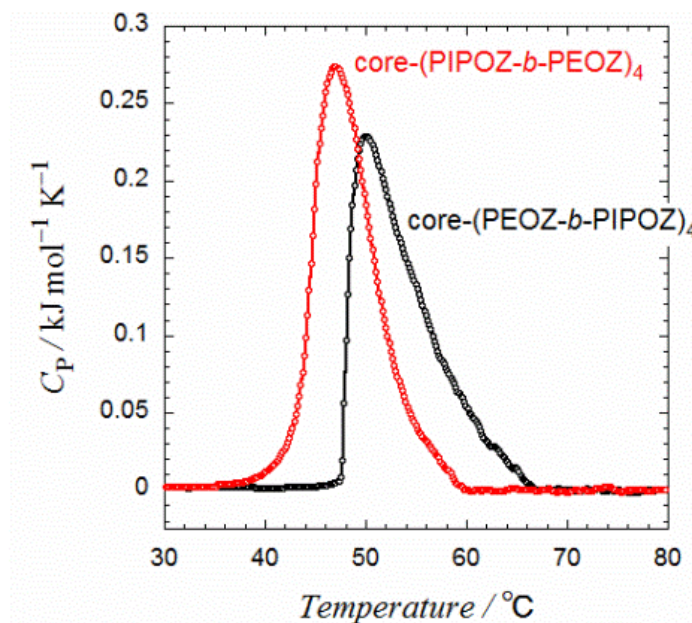


Figure 2. HS-DSC thermograms of aqueous solutions of core-(PEOZ-*b*-PIPOZ)₄ (black trace and core-(PIPOZ-*b*-PEOZ)₄ (red trace); polymer concentration: 2.0 g/L; heating rate: 1.0 °C/min.

Determination of the cloud point of aqueous tetra-arm star copolymers in water. The temperature dependence of the transmittance at 550 nm of aqueous solutions of the two star block copolymers are presented in Figure 3, together with the transmittance data recorded for the starting diblock copolymers. Sato-san: I suggest we move here the data now in SI. The solutions cloud points, taken as the temperature corresponding to the sharp decrease in solution transmittance, are slightly lower than the temperatures T_m derived from the endotherms recorded by HS-DSC (Figure 2), as observed in previous studies of aqueous amphiphilic polymer solutions.

Temperature induced liquid/liquid phase separation of aqueous tetra-arm star copolymers in water. When aqueous solutions of core-(PIPOZ-*b*-PEOZ)₄ and core-(PEOZ-*b*-PIPOZ)₄ with $w = 0.0244$ are heated at 50 and 60 °C for a few hours, macroscopic phase separation takes place. In Figure 4, we present photographs of aqueous suspensions of core-(PIPOZ-*b*-PEOZ)₄ (left vial) and core-(PEOZ-*b*-PIPOZ)₄ (right vial) kept

at 50 °C (top row) and 60 °C (bottom row) for 240 min. For each temperature, macroscopic phase separation occurs faster in the core-(PEOZ-*b*-PIPOZ)₄ sample, compared to the core-(PIPOZ-*b*-PEOZ)₄ sample. As shown in Figure 2, the peak of the DSC thermogram for the aqueous core-(PEOZ-*b*-PIPOZ)₄ is slightly broader, so that the PEOZ block chain in core-(PEOZ-*b*-PIPOZ)₄ should be more hydrophilic than the PEOZ block chain in core-(PIPOZ-*b*-PEOZ)₄, which may help the coagulation of colloidal concentrated-phase droplets.^{13,18} *The sharpness is related usually to the cooperativity of the transition. The sample hydrophobicity affects T_m or T_c. so I would delete the sentence in red above t.* Macroscopic phase separation was reported in an earlier study of related PIPOZ-*b*-PEOZ aqueous solutions heated at 50 °C for 240 min.¹³ Hence, this characteristic feature of the copolymers is preserved upon linkage to the tetrafunctional core.

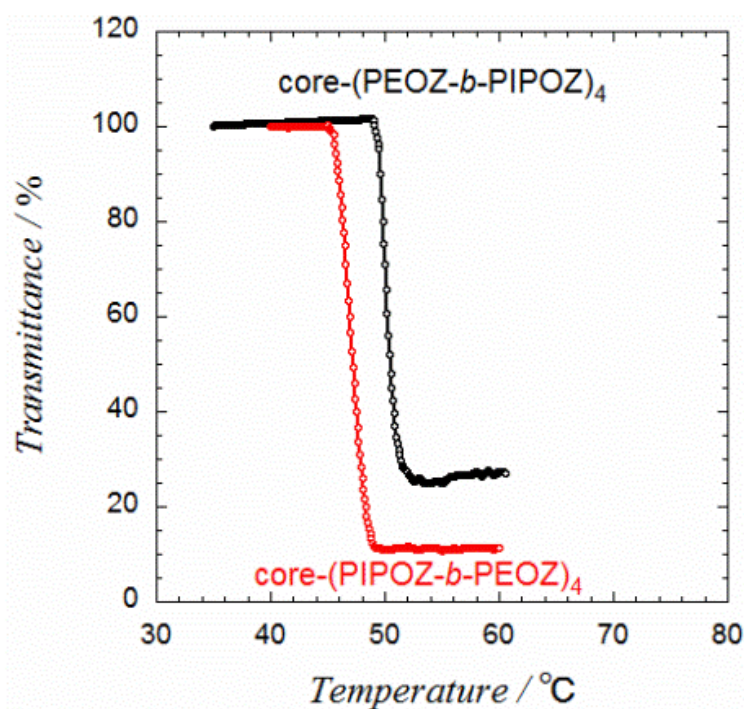


Figure 3. Temperature dependence of the transmittance at 550 nm of aqueous solutions of core-(PIPOZ-*b*-PEOZ)₄ and core-(PEOZ-*b*-PIPOZ)₄; polymer concentration: 1.0 g/L; heating rate: 0.2 °C/min.

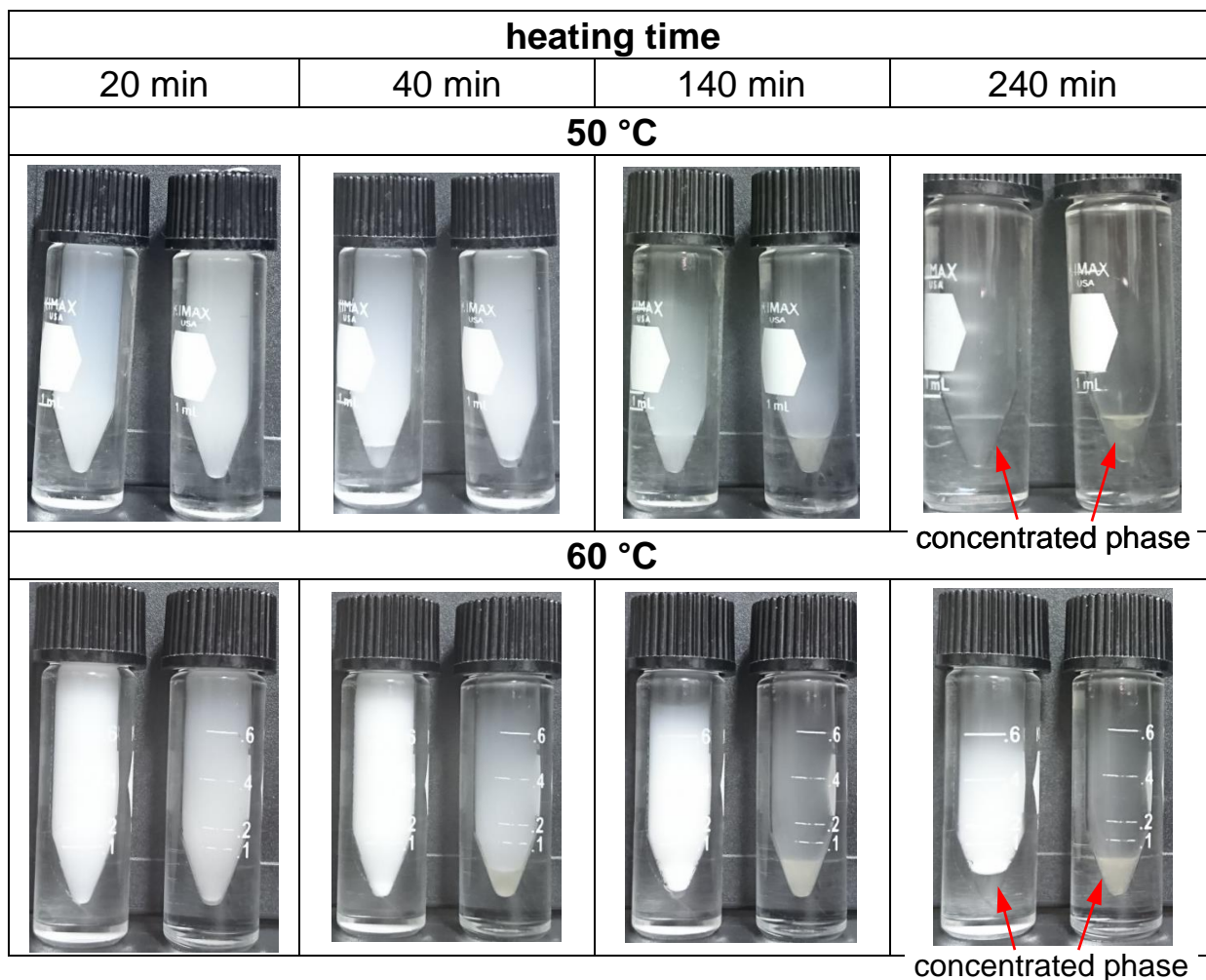


Figure 4. Photographs of phase separating aqueous solutions ($w = 0.0244$) of core-(PIPOZ-*b*-PEOZ)₄ (left vial in each photograph) and core-(PEOZ-*b*-PIPOZ)₄ (right vial in each photograph) heated for prolonged time at 50 °C (top row) and 60 °C (bottom row).

SAXS Profiles. Figure 5 shows SAXS profiles recorded for aqueous solutions of core-(PIPOZ-*b*-PEOZ)₄ and core-(PEOZ-*b*-PIPOZ)₄ ($w = 0.0244$) 3 min after a T-jump to different temperatures. After such a short time, the turbid samples show no sign of macroscopic phase separation. In Panel a, the scattering profile for the aqueous core-(PIPOZ-*b*-PEOZ)₄ shows a plateau at $k < 0.3 \text{ nm}^{-1}$ at 25 °C, and the plateau value increases at 40 and 50 °C. These plateaus indicate that the solutions contain only a small scattering component, and the aggregation number of the small component slightly increases with increasing temperature up to 50 °C. It is noted that the heat capacity in Figure 2 starts

increasing for core-(PIPOZ-*b*-PEOZ)₄ above 40 °C, corresponding to the increase of the scattering plateau value. On the other hand, at 60 and 70 °C, the scattering profile shows an upswing in the low k region, a plateau in the intermediate k region ($0.2 \text{ nm}^{-1} < k < 0.4 \text{ nm}^{-1}$), and a sharp decrease for $k > 0.4 \text{ nm}^{-1}$. These profiles indicate that the solutions contain large and small scattering components.

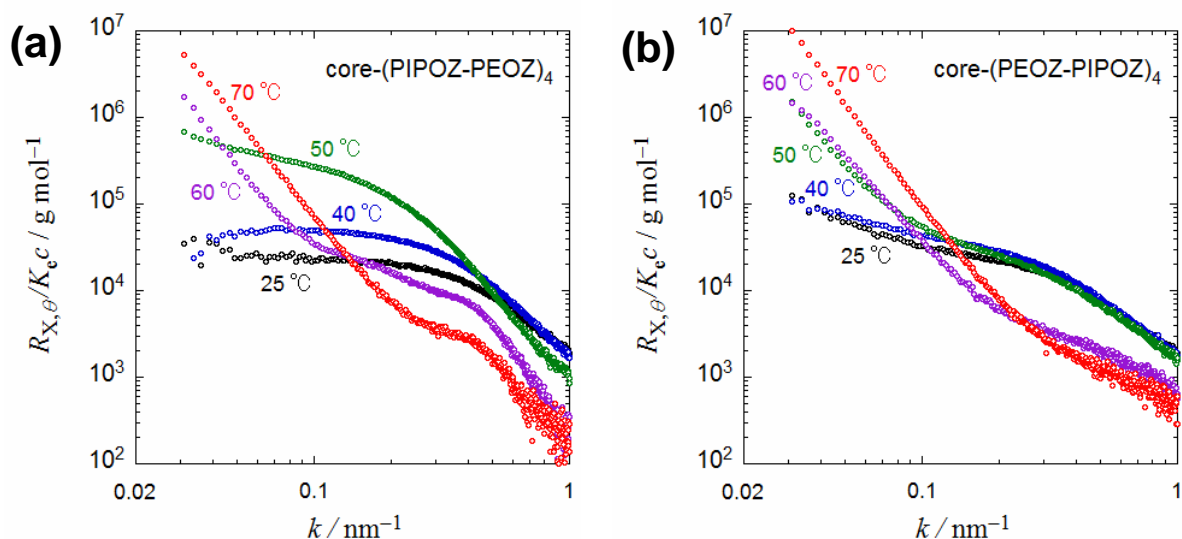


Figure 5. SAXS results for aqueous solutions of (a) core-(PEOZ-*b*-PIPOZ)₄ and (b) core-(PIPOZ-*b*-PEOZ)₄ ($w = 0.0244$) at different temperatures.

In Panel b of Figure 5, the scattering profile for the aqueous core-(PEOZ-*b*-PIPOZ)₄ shows a small upswing in the k region lower than 0.1 nm^{-1} even at 25 °C, and the upswing is enhanced above 50 °C. The scattering intensity decreases in the k region higher than 0.1 nm^{-1} at 60 and 70 °C. The upswing of the scattering function in the low k region indicates the existence of large aggregates in the solution, and the scattering intensity decrease in the high k region demonstrates the decrease of the main component of a small size. As shown in Figure 2, the dehydration starts around 50 °C for core-(PEOZ-*b*-PIPOZ)₄, which corresponds to the scattering profile change. The decay of the scattering intensity at $k > 0.5 \text{ nm}^{-1}$ is markedly sharper for core-(PIPOZ-*b*-PEOZ)₄ in Panel a than core-(PEOZ-*b*-PIPOZ)₄ in Panel b, indicating that the small scattering components of the two star block copolymers takes

different conformations.

Let us discuss the above scattering profiles more quantitatively. At 25 °C, the dehydration does not take place, neither in the case of PIPOZ nor of PEOZ block arm chains. Water is a good solvent for both blocks, so that we may expect that both star block copolymers are molecularly dispersed in water. The scattering function for a molecularly dispersed Gaussian star block copolymer can be calculated by eqs S1-S5 in the Supporting Information. In Figure 6a, the solid curve for core-(PIPOZ-*b*-PEOZ)₄ at 25 °C indicates the = theoretical values for the molecularly dispersed star block-copolymer with a main-chain bond length $b_{\text{PIPOZ}} = b_{\text{PEOZ}} = 0.41$ nm for core-(PIPOZ-*b*-PEOZ)₄. These b values are smaller than the effective bond length estimated to be 0.67 nm [= $(2qh)^{1/2}$] from the persistence length $q = 0.7$ nm^{19, 20} and the contour length per monomer unit $h = 0.32$ nm.²¹ The chain thickness effect on the scattering function may be one of reasons for the underestimate of the b values in the fitting.²²⁻²⁴

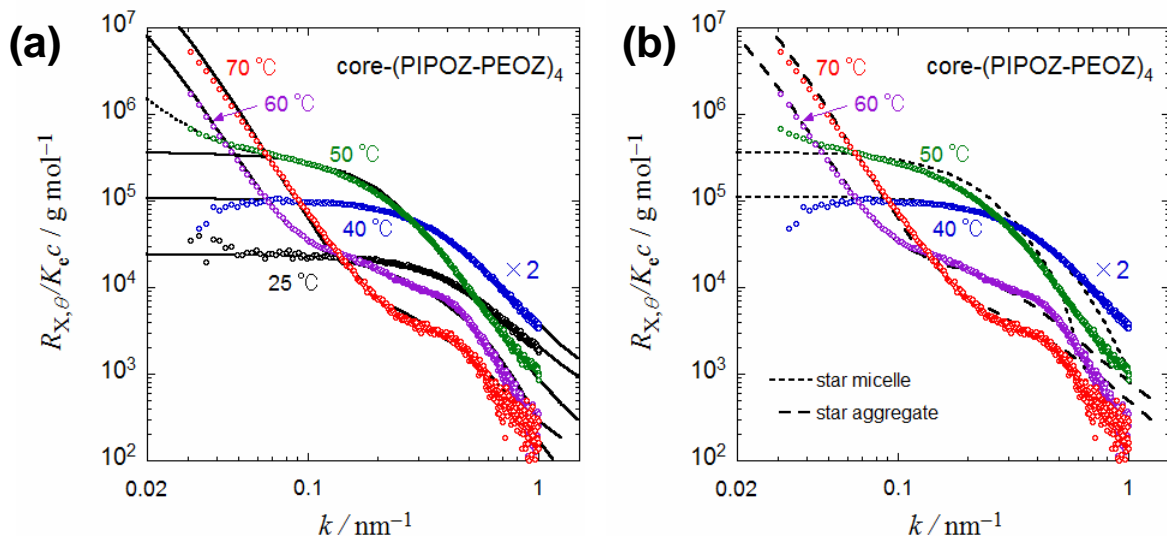
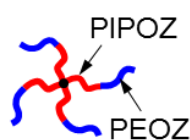


Figure 6. Comparison between theory (curves) and experiment (circles) for the scattering functions of aqueous core-(PIPOZ-*b*-PEOZ)₄ at different temperatures. Panel a shows the best fits, to be compared with less satisfactory fits shown in Panel b. Curves and circles at 40 °C are shifted vertically for viewing clarity.

In Panel a of Figure 5, the plateau value in the low k region increases at 40 and 50 °C, indicating that the isolated star-block copolymer chain aggregates to increase the molar mass

or the aggregation number at 40 and 50 °C. Because the PIPOZ block chain is more hydrophobic than the PEOZ block chain, we can expect for core-(PIPOZ-*b*-PEOZ)₄ to form the star aggregate or star micelle illustrated in Figure 7. Here, the star aggregate means the star polymer of which arm number is equal to the arm number of the original star multiplied by the aggregation number *m*, while the star micelle is the spherical micelle with the hydrophobic core of the uniform density formed by the inner hydrophobic block chains. The scattering functions for the star aggregate and star micelle are given by eqs S1-S5 where *f* is replaced by 4*m* and eqs S7-S9 in the Supporting Information, respectively.

(a) core-(PIPOZ-*b*-PEOZ)₄



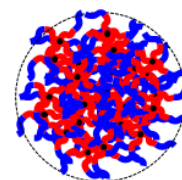
isolated chain



star aggregate

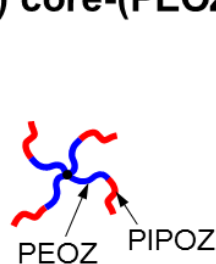


star micelle

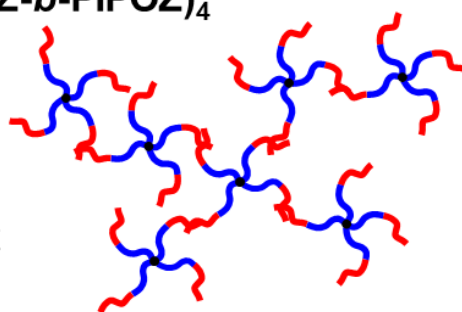


**spherical aggregate
(concentrated-phase droplet)**

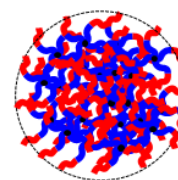
(b) core-(PEOZ-*b*-PIPOZ)₄



isolated chain



random aggregate



**spherical aggregate
(concentrated-phase droplet)**

Figure 7. Schematic diagrams for different types of aggregates formed by star block-copolymers of core-(PIPOZ-*b*-PEOZ)₄ (a) and core-(PEOZ-*b*-PIPOZ)₄ (b).

Solid curves for 40 and 50 °C in Figure 6a represent fitting results by the star aggregate model, calculated by eqs S1-S5. Agreements between theory and experiment are good at $k > 0.05 \text{ nm}^{-1}$. As shown in Panel b of Figure 6, the star micelle model (using eqs S7-S9) gives

the scattering functions at 40 and 50 °C decaying too rapidly at $k > 0.5 \text{ nm}^{-1}$ (dotted curves).

The SAXS scattering functions for core-(PIPOZ-*b*-PEOZ)₄ at 60 and 70 °C shown in Figure 5a show strong upswings in the low k region, that are less pronounced in the high k region, indicating that large scattering component appears while the small scattering component gradually disappears. The scattering function for the solution containing the large and small scattering components may be written as¹³

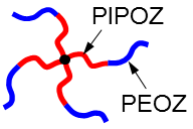
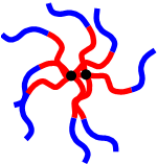
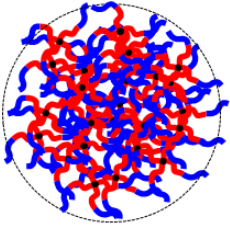
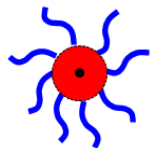
$$\frac{R_{X,\theta}}{K_e c} = M_{w,1} \left[w_{\text{small}} m_{w,\text{small}} P_{\text{small}}(k) + w_{\text{large}} m_{w,\text{large}} P_{\text{large}}(k) \right] \quad (5)$$

where $M_{w,1}$ is the molar mass of a single star block copolymer chain, w_{small} , $m_{w,\text{small}}$ and $P_{\text{small}}(k)$ are the weight fraction (in the total copolymer), the weight-average aggregation number, and the particle scattering function of the small component, and w_{large} , $m_{w,\text{large}}$ and $P_{\text{large}}(k)$ are those of the large aggregated component. The scattering intensity of the large components is predominant only in low k region, and that of the small component contributes mainly in high k region, so that the parameters can be determined separately.

As shown in the previous subsection, macroscopic phase separation takes place in the aqueous solution of core-(PIPOZ-*b*-PEOZ)₄ at 50 and 60 °C. Thus, the large aggregating component in the solution just after the T-jump to 60 and 70 °C must be colloidal droplets of the concentrated phase. The scattering function $P_{\text{sphere}}(k)$ for polydisperse spherical particles of uniform concentration c_{in} given by eq S13 is used for $P_{\text{large}}(k)$ to fit the upswing scattering profiles at 60 and 70 °C in the low k region. When the star micelle model is used for $P_{\text{small}}(k)$, we can fit the profiles at 60 and 70 °C over the entire k region, as shown by solid curves in Figure 6a. The star aggregate model cannot fit the sharply decaying profiles at 60 and 70 °C at $k > 0.5 \text{ nm}^{-1}$, as indicated by dashed curves in Figure 6b.

Table 2. Values of fitting parameters for core-(PIPOZ-*b*-PEOZ)₄ determined by SAXS profiles; $\langle S^2 \rangle_{\text{PIPOZ}}^{1/2}$, $\langle S^2 \rangle_{\text{PEOZ}}^{1/2}$, $\langle S^2 \rangle_{\text{star}}^{1/2}$, and $\langle S^2 \rangle_z$ are the radii of gyration of the PIPOZ and

PEOZ block chains, of the star block copolymer chain, and of the spherical aggregate, respectively, and R_{core} is the radius of the hydrophobic core of the star micelle (cf. the Supporting Information).

Temperature	Component	w	m_w	Remarks
25 °C	 isolated star	1	1	$b_{\text{IPOZ}} = b_{\text{EOZ}} = 0.41 \text{ nm}$ $\langle S^2 \rangle_{\text{PIPOZ}}^{1/2} = 1.9 \text{ nm}$, $\langle S^2 \rangle_{\text{PEOZ}}^{1/2} = 1.6 \text{ nm}$, $\langle S^2 \rangle_{\text{star}}^{1/2} = 4.0 \text{ nm}$
40 °C	 star aggregate	1	2.2	$b_{\text{IPOZ}} = b_{\text{EOZ}} = 0.48 \text{ nm}$ $\langle S^2 \rangle_{\text{PIPOZ}}^{1/2} = 2.3 \text{ nm}$, $\langle S^2 \rangle_{\text{PEOZ}}^{1/2} = 1.9 \text{ nm}$, $\langle S^2 \rangle_{\text{star}}^{1/2} = 4.9 \text{ nm}$
50 °C	star aggregate	0.993	15	$b_{\text{IPOZ}} = b_{\text{EOZ}} = 0.87 \text{ nm}$ $\langle S^2 \rangle_{\text{PIPOZ}}^{1/2} = 4.1 \text{ nm}$, $\langle S^2 \rangle_{\text{PEOZ}}^{1/2} = 3.4 \text{ nm}$, $\langle S^2 \rangle_{\text{star}}^{1/2} = 9.2 \text{ nm}$
	 spherical aggregate	0.007	5.0×10^4	$m_{w,\text{small}}/m_{n,\text{small}} = 20$ $c_{\text{in}} = 0.24 \text{ g/cm}^3$, $\langle S^2 \rangle_z = 220 \text{ nm}$
60 °C	 star micelle	0.43	2	$c_{\text{core}} = 0.18 \text{ g/cm}^3$, $R_{\text{core}} = 4.0 \text{ nm}$ $b_{\text{EOZ}} = 0.47 \text{ nm}$
	spherical aggregate	0.57	3.0×10^5	$m_{w,\text{small}}/m_{n,\text{small}} = 30$ $c_{\text{in}} = 0.04 \text{ g/cm}^3$, $\langle S^2 \rangle_z = 830 \text{ nm}$
70 °C	star micelle	0.09	2	$c_{\text{core}} = 0.35 \text{ g/cm}^3$, $R_{\text{core}} = 3.2 \text{ nm}$ $b_{\text{EOZ}} = 0.30 \text{ nm}$
	spherical aggregate	0.91	1.5×10^5	$m_{w,\text{small}}/m_{n,\text{small}} = 100$ $c_{\text{in}} = 0.042 \text{ g/cm}^3$, $\langle S^2 \rangle_z = 900 \text{ nm}$

The scattering profile for core-(PIPOZ-*b*-PEOZ)₄ at 50 °C in Figure 6a has also a weak upswing in the low k region. As indicated by the dotted curve in Figure 6a, the addition of a

tiny amount of colloidal droplets of the concentrated phase to the star aggregate model fits better in the low k region. Fitting parameters used for the profiles of aqueous core-(PIPOZ-*b*-PEOZ)₄ at different temperatures are summarized in Table 2.

Scattering profiles for the aqueous solution of core-(PEOZ-*b*-PIPOZ)₄ at different temperatures shown in Figure 5b are fitted similarly. The solid curve at 25 °C in Figure 8 indicates the fitting result by the molecularly dispersed star block-copolymer with the main-chain bond lengths $b_{\text{IPOZ}} = b_{\text{EOZ}} = 0.43$ nm for core-(PEOZ-*b*-PIPOZ)₄. The upswing of the experimental scattering function at $k < 0.1$ nm⁻¹ at 25 °C indicates the contamination of a tiny amount of a large aggregate. Because the dehydration does not take place at 25 °C on the core-(PEOZ-*b*-PIPOZ)₄ chain, the large aggregate may not be the concentrated phase droplet but a random aggregate of the star block copolymer illustrated in Figure 7b. The dotted curve for 25 °C in Figure 8 shows the fitting result by the model of a mixture of the isolated chain and random aggregate, using eq 5 along with eqs S10 and S11 in the Supporting Information. The weight fraction of the random aggregate is only 0.15 wt%, but the aggregation number is as high as 1.3×10^5 , so that the scattering power of the aggregate is very strong. Similar enhanced low angle scattering was observed in dilute solutions of thermosensitive linear homopolymers and block copolymers in good solvents,^{25, 26} although the reason for the large aggregate formation in good solvents remains to be seen.

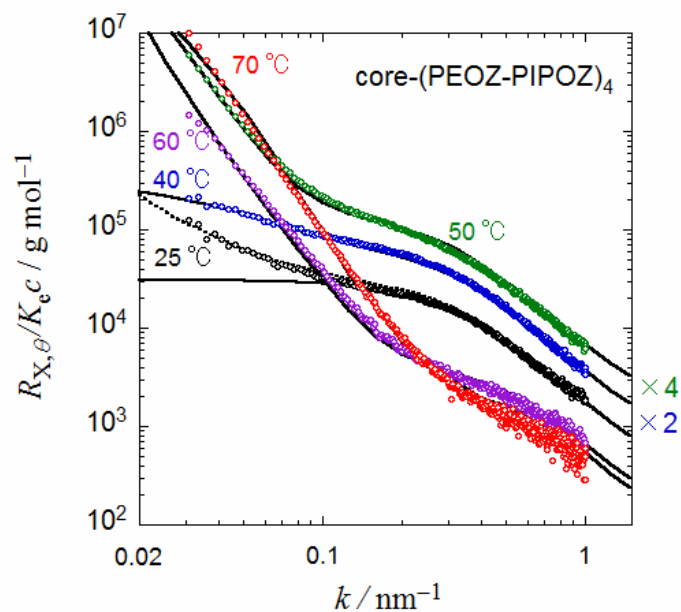
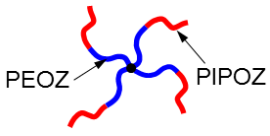
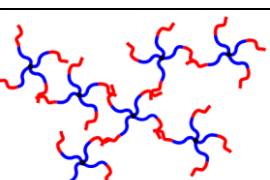
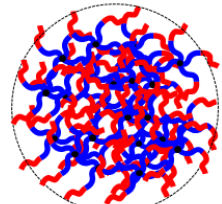


Figure 8. Comparison between theory (curves) and experiment (circles) for the scattering functions of aqueous core-(PEOZ-*b*-PIPOZ)₄ at different temperatures. Curves and circles at 40 and 50 °C are shifted vertically for viewing clarity.

The scattering profile at 40 °C can be fitted by the same mixture model of the isolated chain and random aggregate, although the aggregation number of the random aggregate ($= 1.3 \times 10^3$) is much smaller than that at 25 °C. The upswing of the scattering profiles at 50 – 70 °C may be attributed to colloidal droplets of the concentrated phase, as in the case of core-(PIPOZ-*b*-PEOZ)₄. To the small scattering component, we can assign the isolated star over all temperatures examined, although the aggregation number only at 50 °C should be chosen to be slightly larger than unity ($= 1.25$). The good fitting results are shown by solid curves in Figure 8, and the fitting parameters determined are listed in Table 3. The monomer unit lengths b_{EOZ} and b_{IPOZ} at 60 and 70 °C are considerably smaller than the expected ($= 0.67$ nm; see above), which may reflect the shrinkage of the copolymer chain due to dehydration (cf. Figure 2).

Table 3. Values of fitting parameters for core-(PEOZ-*b*-PIPOZ)₄ determined by SAXS profiles; $\langle S^2 \rangle_{\text{PIPOZ}}^{1/2}$, $\langle S^2 \rangle_{\text{PEOZ}}^{1/2}$, $\langle S^2 \rangle_{\text{star}}^{1/2}$, and $\langle S^2 \rangle_z$ are the radii of gyration of the PIPOZ and PEOZ block chains, of the star block copolymer chain, and of the spherical aggregate, respectively, and R_{core} is the radius of the hydrophobic core of the star micelle (cf. the Supporting Information).

Temperature	Component	w	m_w	Remarks
25 °C	 isolated star	0.999	1	$b_{\text{EOZ}} = b_{\text{IPOZ}} = 0.43 \text{ nm}$ $\langle S^2 \rangle_{\text{PEOZ}}^{1/2} = 2.3 \text{ nm}$, $\langle S^2 \rangle_{\text{PIPOZ}}^{1/2} = 2.0 \text{ nm}$, $\langle S^2 \rangle_{\text{star}}^{1/2} = 4.8 \text{ nm}$
	 random aggregate	0.001	1.3×10^5	$b = 2 \text{ nm}$, $\langle S^2 \rangle_{\text{agg}}^{1/2} = 450 \text{ nm}$
40 °C	isolated star	0.997	1	$b_{\text{EOZ}} = b_{\text{IPOZ}} = 0.42 \text{ nm}$ $\langle S^2 \rangle_{\text{PEOZ}}^{1/2} = 2.2 \text{ nm}$, $\langle S^2 \rangle_{\text{PIPOZ}}^{1/2} = 1.9 \text{ nm}$, $\langle S^2 \rangle_{\text{star}}^{1/2} = 4.7 \text{ nm}$
	random aggregate	0.003	1.3×10^3	$b = 2 \text{ nm}$, $\langle S^2 \rangle_{\text{agg}}^{1/2} = 45 \text{ nm}$
50 °C	isolated star	0.92	1.25	$b_{\text{EOZ}} = 0.5 \text{ nm}$, $b_{\text{IPOZ}} = 0.4 \text{ nm}$ $\langle S^2 \rangle_{\text{PEOZ}}^{1/2} = 2.7 \text{ nm}$, $\langle S^2 \rangle_{\text{PIPOZ}}^{1/2} = 1.8 \text{ nm}$
	 spherical aggregate	0.08	1.5×10^5	$m_{w,\text{small}}/m_{n,\text{small}} = 100$ $c_{\text{in}} = 0.1 \text{ g/cm}^3$, $\langle S^2 \rangle_z = 730 \text{ nm}$
60 °C	isolated star	0.14	1	$b_{\text{EOZ}} = b_{\text{IPOZ}} = 0.27 \text{ nm}$ $\langle S^2 \rangle_{\text{PEOZ}}^{1/2} = 1.4 \text{ nm}$, $\langle S^2 \rangle_{\text{PIPOZ}}^{1/2} = 1.2 \text{ nm}$, $\langle S^2 \rangle_{\text{star}}^{1/2} = 3.0 \text{ nm}$
	spherical aggregate	0.86	1.9×10^5	$m_{w,\text{small}}/m_{n,\text{small}} = 4.6$ $c_{\text{in}} = 0.05 \text{ g/cm}^3$, $\langle S^2 \rangle_z = 430 \text{ nm}$
70 °C	isolated star	0.08	1	$b_{\text{EOZ}} = b_{\text{IPOZ}} = 0.23 \text{ nm}$ $\langle S^2 \rangle_{\text{PEOZ}}^{1/2} = 1.2 \text{ nm}$, $\langle S^2 \rangle_{\text{PIPOZ}}^{1/2}$

				$= 1.0 \text{ nm}, \langle S^2 \rangle_{\text{star}}^{1/2} = 2.5 \text{ nm}$
	spherical aggregate	0.92	5.0×10^3	$m_{w,\text{small}}/m_{n,\text{small}} = 20$ $c_{\text{in}} = 0.04 \text{ g/cm}^3, \langle S^2 \rangle_z = 210 \text{ nm}$

CONCLUSIONS

The dependence on molecular architecture of the dehydration, phase separation, and micellization behavior were investigated for aqueous solutions of thermosensitive polyoxazoline star block copolymers. Two star block copolymers, core-(PIPOZ-*b*-PEOZ)₄ and core-(PEOZ-*b*-PIPOZ)₄, where more hydrophobic PIPOZ block chains are inside and outside the star block copolymer respectively, were synthesized, and their dilute aqueous solutions were examined by HS-DSC, turbidity, and SAXS measurements. The dehydration and phase separation behavior is not so much different for the two star block copolymers with opposite an architecture. However, the micellization behavior is remarkably different for the two star block copolymers. The PIPOZ blocks inside core-(PIPOZ-*b*-PEOZ)₄ trigger the formation of the star micelles in water upon heating. However, core-(PEOZ-*b*-PIPOZ)₄ exists as the isolated chains in water even at high temperatures, possibly because the collapsed PIPOZ blocks on the periphery of the star remain separated from each other by PEOZ loops and cannot aggregate.

ACKNOWLEDGEMENT

The synchrotron radiation experiments were performed at the BL40B2 in SPring-8 with the approval of the Japan Synchrotron Radiation Research Institute (JASRI) (Proposal No 2017B1409). We thank Dr. K. Terao at Osaka University for helping with the SAXS measurements. This work was supported in part by JSPS KAKENHI Grant No. 18H02020.

REFERENCES

1. Ren, J. M.; McKenzie, T. G.; Fu, Q.; Wong, E. H. H.; Xu, J.; An, Z.; Shanmugam, S.;

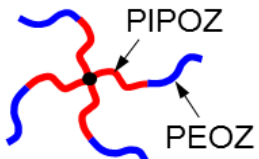
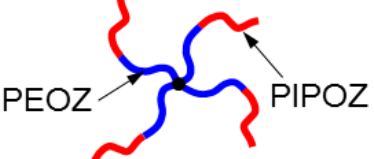
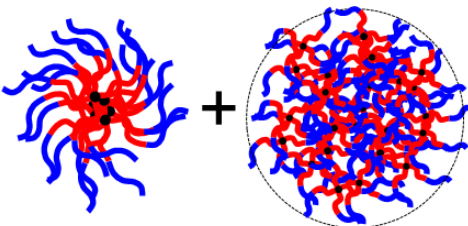
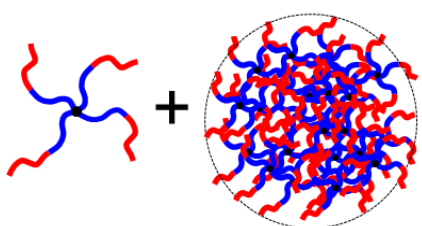
- Davis, T. P.; Boyer, C.; Qiao, G. G. *Chem. Rev.* **2016**, 116, 6743-6836.
2. Qiu, N.; Li, Y.; Li, Y.; Wang, H.; Duan, Q.; Kakuchi, T. *RSC Adv.* **2016**, 6, 47912-47918.
 3. Takamizu, K.; Nomura, K. *J. Am. Chem. Soc.* **2012**, 134, 7892-7895.
 4. Libera, M.; Trzebicka, B.; Kowalczyk, A.; Wałach, W.; Dworak, A. *Polymer* **2011**, 52, 250-257.
 5. Qu, Y.; Chang, X.; Chen, S.; Zhang, W. *Polym. Chem.* **2017**, 8, 3485-3496.
 6. Zhou, J.; Wang, L.; Ma, J.; Wang, J.; Yu, H.; Xiao, A. *European Polym. J.* **2010**, 46, 1288-1298.
 7. Sánchez-Bustos, E.; Cornejo-Bravo, J.; Licea-Claverie, A. *J. Chem.* **2016**, 2016, 4543191.
 8. Tao, K.; Wang, Y.; Wang, W.; Lu, D.; Wang, Y.; Bai, R. *Macromol. Chem. Phys.* **2009**, 210, 478-485.
 9. Strandman, S.; Zarembo, A.; Darinskii, A. A.; Laurinmäki, P.; Butcher, S. J.; Vuorimaa, E.; Lemmetyinen, H.; Tenhu, H. *Macromolecules* **2008**, 41, 8855-8864.
 10. Hu, H.; Liu, G. *Macromolecules* **2014**, 47, 5096-5103.
 11. Tasci, E.; Aydin, M.; Gorur, M.; Gürek, A. G.; Yilmaz, F. *J. PAppl. Polym. Sci.* **2018**, 135, 46310.
 12. Bekhradnia, S.; Diget, J. S.; Zinn, T.; Zhu, K.; Sande, S. A.; Nyström, B.; Lund, R. *Macromolecules* **2015**, 48, 2637-2646.
 13. Takahashi, R.; Sato, T.; Terao, K.; Qiu, X.-P.; Winnik, F. M. *Macromolecules* **2012**, 45, 6111-6119.
 14. Huber, S.; Jordan, R. *Colloid Polym. Sci.* **2008**, 286, 395-402.
 15. Fijten, M. W. M.; Haensch, C.; van Lankvelt, B. M.; Hoogenboom, R.; Schubert, U. S. *Macromol. Chem. Phys.* **2008**, 209, 1887-1895.
 16. Takahashi, R.; Sato, T.; Terao, K.; Yusa, S. *Macromolecules* **2015**, 48, (19), 7222-7229.
 17. Takahashi, R.; Sato, T.; Terao, K.; Yusa, S. *Macromolecules* **2016**, 49, (8), 3091-3099.

18. Takahashi, R.; Qiu, X.-P.; Xue, N.; Sato, T.; Terao, K.; Winnik, F. M. *Macromolecules* **2014**, *47*, 6900-6910
19. Sung, J. H.; Lee, D. C. *Polymer* **2001**, *42*, 5771-5779.
20. Kondo, M.; Takahashi, R.; Qiu, X.-P.; Winnik, F. M.; Terao, K.; Sato, T. *Polym. J.* **2016**, submitted.
21. Litt, A.; Rahl, F.; Roldan, L. G. *J. Polym.Sci.: Part A2* **1969**, *7*, 463-473.
22. Hickl, P.; Ballauff, M.; Scherf, U.; Müllen, K.; Lindner, P. *Macromolecules* **1997**, *30*, (2), 273-279.
23. Terao, T.; Mizuno, K.; Murashima, M.; Kita, Y.; Hongo, C.; Okuyama, K.; Norisuye, T.; Bächinger, H. P. *Macromolecules* **2008**, *41*, (19), 7203-7210.
24. Arakawa, S.; Terao, K.; Kitamura, S.; Sato, T. *Polym. Chem.* **2012**, *3*, 472-478.
25. Kawaguchi, T.; Kobayashi, K.; Osa, M.; Yoshizaki, T. *J. Phys. Chem. B* **2009**, *113*, 5440-5447.
26. Sato, T.; Tanaka, K.; Toyokura, A.; Mori, R.; Takahashi, R.; Terao, K.; Yusa, S. *Macromolecules* **2013**, *46*, 226-235.

Table of Contents Graphic

“Dehydration, Micellization, and Phase Separation of Thermosensitive Polyoxazoline Star Block-Copolymers in Aqueous Solution”

by Tetiana Sezonenko, Xing-Ping Qiu, Françoise M. Winnik, and Takahiro Sato

Temp.	core-(PIPOZ- <i>b</i> -PEOZ) ₄	core-(PEOZ- <i>b</i> -PIPOZ) ₄
25 °C		
50 °C		
60 °C, 70 °C	